Improved Sensor Fault-Tolerant Control Technique Applied to Three-Phase Induction Motor Drive

Minh Chau Huu Nguyen[1], Cuong Dinh Tran[2]
[1]Faculty of Electrical Engineering and Computer Science, VSB-Technical University of Ostrava, Czech Republic
[1]Faculty of Electrical and Electronics Engineering, Vietnam Aviation Academy, Vietnam
[2]Power System Optimization Research Group, Faculty of Electrical and Electronics Engineering, Ton Duc Thang University, Ho Chi Minh City, Vietnam

Article Info

Article history:

Received Oct 30, 2022
Revised May 13, 2023
Accepted Jun 18, 2023

Keywords:

Current sensor fault
Fault-tolerant control
Field-oriented control
Induction motor
Speed sensor fault

ABSTRACT

An improved fault-tolerant control (FTC) method using mathematical functions is applied to the induction motor drive (IMD) against current sensors and speed encoder failures, which occur when the sensor is disconnected or completely damaged. The IMD with two current sensors and an encoder is speed controlled based on the field-oriented control (FOC) technique in regular operation. In this paper, an FTC unit is implemented in the FOC controller to detect and solve the sensor fault to increase the reliability of the speed control process. The measured stator currents and the feedback speed signal are integrated into the diagnosis algorithms to create a sensor fault-tolerant control function. Three diagnosis functions operating in a defined sequence are proposed for determining the health status of current and speed sensors. The FTC function performs isolation and replaces the faulty sensor signals with the proper estimated signals; then, the IMD will operate in the corresponding sensorless mode. Simulations will be performed to verify the accuracy and reliability of the proposed method under various sensor faults.

Corresponding Author:

Cuong Dinh Tran,
Power System Optimization Research Group,
Faculty of Electrical and Electronics Engineering,
Ton Duc Thang University, 19 Nguyen Huu Tho, District 7, Ho Chi Minh City, Vietnam.
Email: trandinhcuong@tdtu.edu.vn

1. INTRODUCTION

The three-phase induction motor (IM) is an AC electric motor that operates on the electromagnetic induction phenomenon to transfer electrical energy into mechanical energy for industrial applications. With the advantages of structure, powerful features, and high efficiency in operation, IM is one of the most used engines in many fields of industry and transportation [1], [2]. In the early days of its inception, IM was mainly used in fixed-speed applications; today, with the rapid development of the field of power electronics, induction motors have extensive involvement in precision speed control.

Two main groups of strategies are used in the speed control of induction motors: scalar control and vector control. Generally, scalar control corresponding to low-cost drive structures is used in applications that do not require high accuracy [3-5]. As opposed to the scalar method, the FOC method corresponding to a high-performance drive structure is established as an engineering solution for speed precision control applications [6-8]. Learning based on the control principle of separately excited DC motors, rotor flux and electrical torque components are separated and controlled independently in the FOC strategy. A motor drive applying the typical FOC strategy has four main components, including the motor, controller, converter, and sensors, illustrated in Figure 1. Through the control structure of the drive using the FOC control method, we can recognize the critical role of the sensor's feedback signals in controlling IMD's motor speed. During operation, if the loss of feedback signal due to damaged sensors occurs, it will lead to the failure of the FOC algorithm in controlling the motor speed [9-11]. Nowadays, to increase the IMD's reliability, FTC techniques have been researched to integrate into the FOC loop to ensure continuous operation even in the event of sensor failure [12], [13]. This paper will analyze and provide an effective FTC solution against failures of the speed encoder and the current sensors. FTC consists of three main processes, performed in sequence, including diagnosing the fault sensors, performing faulty measured signals isolation, and replacing the fault signals with the virtual signs of sensorless techniques. Researchers have published many results on the FTC technique with diverse approaches in many scientific papers.

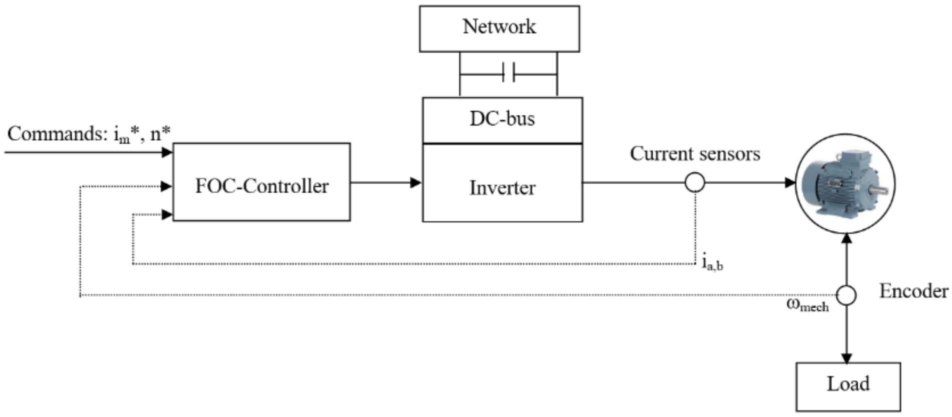

Figure 1. Block diagram of typical FOC drive structure

Article [14] presents the sensor fault diagnosis based on rotor resistance observer and current indexes to detect the falses of sensors in IMD. After the fault is identified, the FTC controller isolates the wrong measured signals and applies the appropriate sensorless technique to keep the operation of the drive. This method is highly accurate; however, since the sampling cycle is carried out in an electrical current cycle, this method's performance is not suitable for low-speed controlling applications. The authors in the article [15] propose an approach based on the Axes transformation technique for a current sensor failure diagnosis method. Measured stator currents establish two observers in the stationary coordinate systems, each shifting 120 degrees. The current element on the α-axis of each measured observer will be compared with the α-element of the two estimated observers. The deviation of elements in observers will indicate the health status of the current sensors. The authors use the typical comparison technique between the virtual speed and the measured value of the encoder to determine a speed sensor fault. In [16], the authors present a method without using the model and parameter machine for the FTC technique in IMD using a FOC loop. An asymmetry factor based on the RMS value of phase stator currents is used for detecting the faulty current sensor. In a FOC loop, reference currents combining measured currents in the rotating coordinate are used as the detection function for diagnosing the fault of the encoder. This method is highly effective in diagnosing and compensating for sensor faults in IMD systems applying the FOC technique. In [17], a method using the rotor flux value and stator currents for a diagnosis algorithm to detect the fault of the encoder in IMD. This method separates the two stages of error diagnosis and reconfiguration into two independent processes that facilitate their independent development. Paper [18] proposes a solution to diagnose open circuit faults of the current and speed sensors based on third-difference operators combining the rotor slip algorithm. The open circuit fault of current sensors is prioritized to analyze first, then continue to check the condition of the speed sensor. The advantage of this technique is the fast diagnostic time and avoids the effects of random noises.

After correctly identifying the faulty sensor, FTC will isolate uncertain feedback signals and apply appropriate sensorless techniques, including speed sensorless [19-22] and current sensorless [23-27], to maintain IMD's operation. In this paper, in order to improve the stability, an improved FTC technique applying mathematical functions for diagnosing the operating status of sensors is integrated with the controller of IMD against the total current and speed sensor faults. The content of the proposed method will be presented in the second section, and the simulation results will be described in the third section. Finally, the fourth part will discuss the method's advantages and disadvantages.

2. PROPOSED FAULT-TOLERANT CONTROL METHOD

In the second section, an improved FTC function integrated into the FOC controller is proposed to reinforce the reliability and stability of IMD against the single fault occurring by disconnection or complete damage of the sensors.

2.1. Nonlinear model of the induction machine

State variables such as currents and magnetic fluxes of the IM motor in [α-β] stationary coordinate system follow the differential equations (1), (2), (3), (4).

$$\boldsymbol{u}_s^S = R_s \boldsymbol{i}_s^S + \frac{d\boldsymbol{\Psi}_s^S}{dt} \quad (1)$$

$$0 = R_r \boldsymbol{i}_r^S - jp\omega_m \boldsymbol{\Psi}_r^S + \frac{d\boldsymbol{\Psi}_r^S}{dt} \quad (2)$$

$$\boldsymbol{\Psi}_s^S = L_s \boldsymbol{i}_s^S + L_m \boldsymbol{i}_r^S \quad (3)$$

$$\boldsymbol{\Psi}_r^S = L_r \boldsymbol{i}_r^S + L_m \boldsymbol{i}_s^S \quad (4)$$

Where $\boldsymbol{u}_s^S$: the input voltage vector, $\boldsymbol{i}_s^S / \boldsymbol{i}_r^S$: the stator and rotor current vectors; $\boldsymbol{\Psi}_s^S / \boldsymbol{\Psi}_r^S$: the stator and rotor flux vectors; ω_m: mechanical motor speed; Rs/Rr: stator and rotor resistances; $L_m/L_s/L_r$: magnetizing, stator, and rotor inductances; p: No. pole pairs.

This paper applies the FOC method with independent magnetic flux and torque control to the IMD drive system. The IMD consists of two current sensors and an encoder powered by a voltage source inverter for speed control, corresponding to Figure 2 [28].

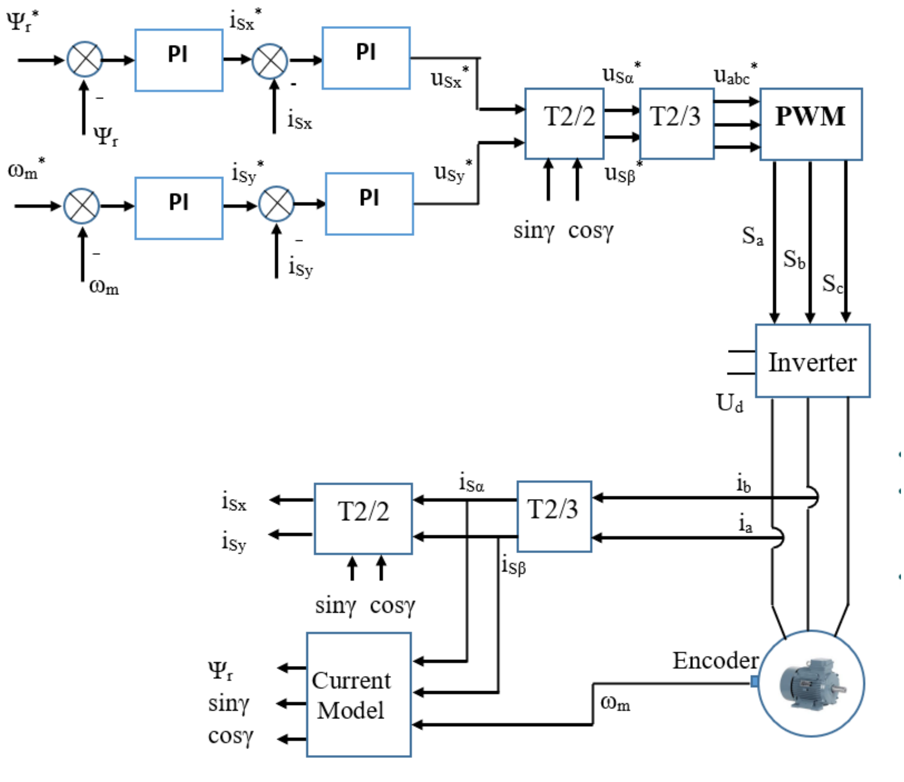

Figure 2. Block diagram of an IMD drive applying FOC method

By applying Clark-Park's formulas, the measured currents are transferred into [α-β] stationary and [x-y] rotation coordinates (5), (6) to provide feedback to the FOC control loop.

$$\text{Clark's equation: } \begin{bmatrix} i_{S\alpha} \\ i_{S\beta} \end{bmatrix} = \begin{bmatrix} 1 & 0 \\ \frac{1}{\sqrt{3}} & \frac{2}{\sqrt{3}} \end{bmatrix} \begin{bmatrix} i_a \\ i_b \end{bmatrix} \quad (5)$$

$$\text{Park's equation: } \begin{bmatrix} i_{Sx} \\ i_{Sy} \end{bmatrix} = \begin{bmatrix} \cos\gamma & \sin\gamma \\ -\sin\gamma & \cos\gamma \end{bmatrix} \begin{bmatrix} i_{S\alpha} \\ i_{S\beta} \end{bmatrix} \quad (6)$$

Where "γ": rotor flux angular.

The current components "$i_{S\alpha}$, $i_{S\beta}$" combined with the measured rotor speed "ω_m" are also used to calculate the rotor flux by the current model.

$$\begin{bmatrix} i_{Sd} \\ i_{Sq} \end{bmatrix} = \begin{bmatrix} \cos\varsigma & \sin\varsigma \\ -\sin\varsigma & \cos\varsigma \end{bmatrix} \begin{bmatrix} i_{S\alpha} \\ i_{S\beta} \end{bmatrix} \tag{7}$$

With: $\varsigma = \int \omega_r dt$, corresponding to rotor angular

$$\begin{bmatrix} i_{mgd} \\ i_{mgq} \end{bmatrix} = \begin{bmatrix} \frac{1}{T_R s+1} & 0 \\ 0 & \frac{1}{T_R s+1} \end{bmatrix} \begin{bmatrix} i_{Sd} \\ i_{Sq} \end{bmatrix} \tag{8}$$

$$\begin{bmatrix} i_{mg\alpha} \\ i_{mg\beta} \end{bmatrix} = \begin{bmatrix} \cos\varsigma & -\sin\varsigma \\ \sin\varsigma & \cos\varsigma \end{bmatrix} \begin{bmatrix} i_{mgd} \\ i_{mgq} \end{bmatrix} \tag{9}$$

$$\begin{cases} \gamma = arctg(\frac{i_{mg\beta}}{i_{mg\alpha}}) \\ i_{mg} = \sqrt{(i_{mg\alpha}^2 + i_{mg\beta}^2)} \\ \psi_r = L_m i_{mg} \end{cases} \tag{10}$$

Where "i_{mg}": magnetic current, "$T_R=L_r/R_r$": rotor time constant

The feedback signals are sent to the FOC control loop to compare with setting values, thereby providing a control voltage signal to the PWM modulator. Then, the PWM modulator will provide switching pulses to an inverter for controlling the motor following the reference speed.

2.2. The proposed fault-tolerant control against the total sensor faults

To improve the reliability and sustain of the IMD against the total sensor fault, which occurs when the sensor is disconnected or completely damaged, a fault detection-isolation (FDI) unit is embedded into a FOC loop for determining the operating states of the IM; Figure 3 shows the structure diagram of IMD integrating the FTC function in the FOC-loop for speed control.

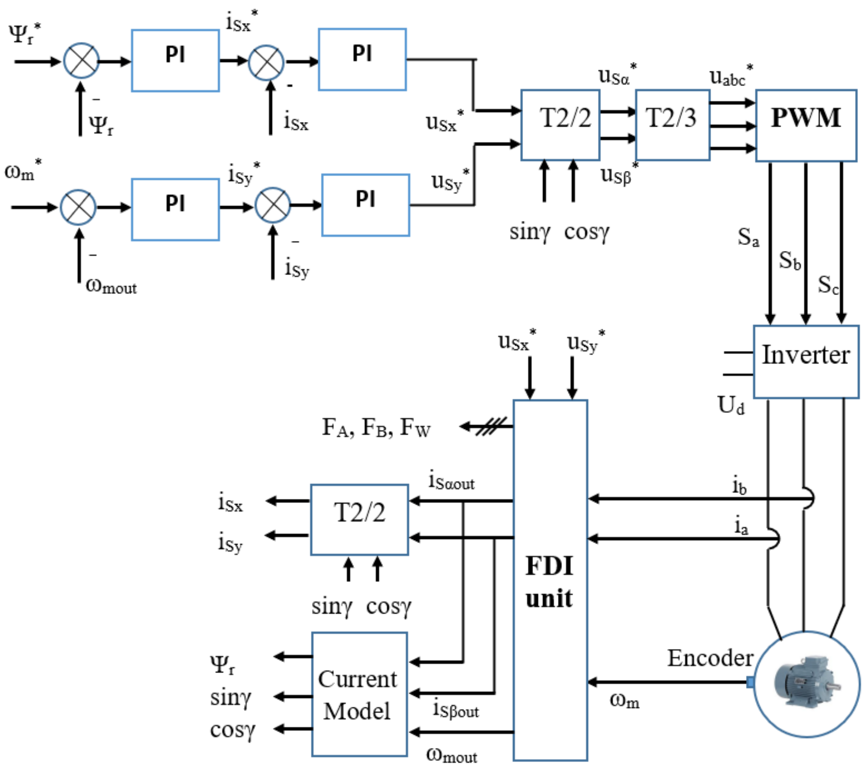

Figure 3. Block diagram of an IMD drive applying FTC based on FOC method

The measured signals from sensors, including stator currents and an encoder, are feedback to the FDI unit for evaluating the quality of signals for deciding on the healthy of the sensors, then provide the output signals to the FOC loop for speed control.

Two diagnosis functions based on measured currents in (11) are used to check the quality of the current signals from the sensors.

$$\begin{cases} Func\_FA = \left| i_a^2 + i_{a\_delay}^2 \right| \\ Func\_FB = \left| i_b^2 + i_{b\_delay}^2 \right| \end{cases} \quad (11)$$

Where:

$i_{a\_delay} = i_a : Delay[Ti];$

$i_{b\_delay} = i_b : Delay[Ti];$

$$\begin{cases} If\ (Func\_FA = 0) \\ \{F_A = 1;\} \\ If\ (Func\_FB = 0) \\ \{F_B = 1;\} \end{cases} \quad (12)$$

Under normal operating conditions, the value of Func_FA and Func_FB is always greater than zero. However, if a total current sensor fault occurs, the values of Func_FA and Func_FB corresponding to each current sensor will equal zero, and the fault flags (F_A and F_B) will increase to a high level (12). “Ti” is a reasonable period for Func_FA and Func_FB to detect the current fault in time, and “Ti” can be selected at about 2 ms, according to [18]. The health of the current signals is determined via the “F_i” flag (13). When current signals are in a healthy state, “F_i” will be 1; otherwise, “F_i” is zero when any current sensor fails.

$$F_i = \overline{F}_A \wedge \overline{F}_B \quad (13)$$

After the condition of the current sensor is determined, the FDI unit applies a diagnosis process to check the health status of the speed sensor corresponding to the formula (14), (15) ref to [17].

$$Func\_FW = \frac{L_m}{T_R.(\psi_{R\alpha}^2 + \psi_{R\beta}^2)}[(i_{S\alpha} - \hat{i}_{S\alpha}).\psi_{R\beta} + (\hat{i}_{S\beta} - i_{S\beta}).\psi_{R\alpha}] \quad (14)$$

$$\begin{cases} If\ (Func\_FW \geq Threshold\_w) \\ \{F_{Wte} = 1;\} \\ F_{Wte\_delay} = F_{Wte} : Delay[Tw] \end{cases} \quad (15)$$

Where: “Tw” is a reasonable period for Func_FW to detect the speed senor fault in time, and “Tw” must be greater than “Ti.” And “Tw” can be selected at about 3.5 ms, according to [18]. “Threshold_w” is the limitation deviation of the real speed and measured speed in the normal operating condition.

The FW flag determines the health status of the measured speed as in formula (16). If the total speed sensor fault occurs, the fault flags (F_W) will increase to a high level.

$$F_W = F_{Wte} \wedge F_{Wte\_delay} \wedge F_i \quad (16)$$

The fault flags’ status and the FDI’s corresponding output are indicated in Table 1.

Table 1. FDI: Logic principle

Fault indication flags	Diagnosis status	Output-FDI
F_A=0, F_B=0, F_W=0	Healthy status	ω_m, $i_{S\alpha}$, $i_{S\beta}$
F_A=0, F_B=0, F_W=1	Speed encoder fault	$\widehat{\omega}$, $i_{S\alpha}$, $i_{S\beta}$
F_A=1, F_B=0, F_W=0	Current sensor fault in A-phase	ω_m, $\widehat{i_{S\alpha}}$, $\widehat{i_{S\beta}}$
F_A=0, F_B=1, F_W=0	Current sensor fault in B-phase	ω_m, $\widehat{i_{S\alpha}}$, $\widehat{i_{S\beta}}$

The estimated signals can be implemented by applying suitable methods such as MRAS, Sliding mode observer (SMO),.. [19-22] for the estimated speed ($\widehat{\omega}$); and machine modeling, Luenberger Observer (LO),.. [23-27] for the estimated current ($\widehat{i_{S\alpha}}$, $\widehat{i_{S\beta}}$). This paper applies the SMO and LO methods to simulate the estimated signals, and these sensorless techniques have been verified for stability by the Lyapunov function in the reference.

3. RESULTS AND DISCUSSION

In order to demonstrate the feasibility and efficiency achieved in enhancing the reliability of the IMD, simulation analyses will be performed under various sensor fault cases. The motor parameters used in simulation models are presented in Table 2:

Table 2. The motor parameters

Description	Value (unit)
Rated Speed/Torque: ω_n/T_n	1420 (rpm) /14.8 (Nm)
Rated current: I_n	4.85 (A)
Stator/Rotor Resistance: R_S/R_R	3.179/2.118 (Ω)
Magnetizing/Stator/Rotor Inductance: $L_m/L_S/L_R$	0.192/0.209/0.209 (H)
No. pole pairs: p	2

The reference speed of the IMD is kept at zero until 0.5 s, then increases to 750 rpm as a step function, as shown in Figure 4(a). Even though the presence of zero speed last 0.5 seconds and the sudden acceleration of the step function, the FTC function of the FDI unit still implements correctly. There is no confusion in sensor fault detection, and all the fault indication flag remains low during this regular operation.

In the first simulation, a complete failure of the speed encoder occurred at 1 second, and the value of this feedback signal fell to zero immediately, Figure 4(a). The FDI unit applied the diagnosis process based on equations from (11) to (16) to detect speed sensor failure correctly, as shown in Figure 4(b). Corresponding to the second case of Table 1, the output signal of the FDI unit supplied to the FOC control loop is the measured currents and the virtual rotor speed, Figure 4(c). The rotor speed fluctuates during the detection and conversion of the control signal, then quickly stabilizes and maintains regular operation. In the second simulation, a complete failure of a current sensor corresponding to the A-phase occurred at 1.5 seconds, and its value fell to zero immediately, Figure 5(a). Similar to the above speed encoder fault, the FTC function of the FDI unit worked correctly, the "F_A" flag increased to a high level, and the other two indication flags remained low, Figure 5(b). Corresponding to the third case of Table 1, the output signals of the FDI unit supplied to the FOC loop are estimated currents and the measured speed, Figure 5(c). The IMD still operates stably, as in Figure 5(d). Although there is a noise pulse of the output current in the conversion process, the IMD system overcomes the transient oscillation and stabilizes quickly. Similar to the second case, the B-phase current sensor fault is simulated in the third case to verify the effectiveness of the proposed FTC solution. The defect occurs with the B-phase measured current at 1.5 s, corresponding to a zero value, as shown in Figure 6(a). The detection and isolation process of the FDI unit still operates correctly, and the B-phase current sensor fault is determined instantaneously, illustrated in Figure 6(b). The output of the FDI unit and the stable operation of the motor are presented in Figures 6(c) and 6(d).

Based on the simulation results, the effectiveness of the proposed solution is demonstrated in accurately detecting and isolating each sensor fault. The FDI unit has provided reasonable control signals to sustain the stable operation of the IMD when sensor failures occur.

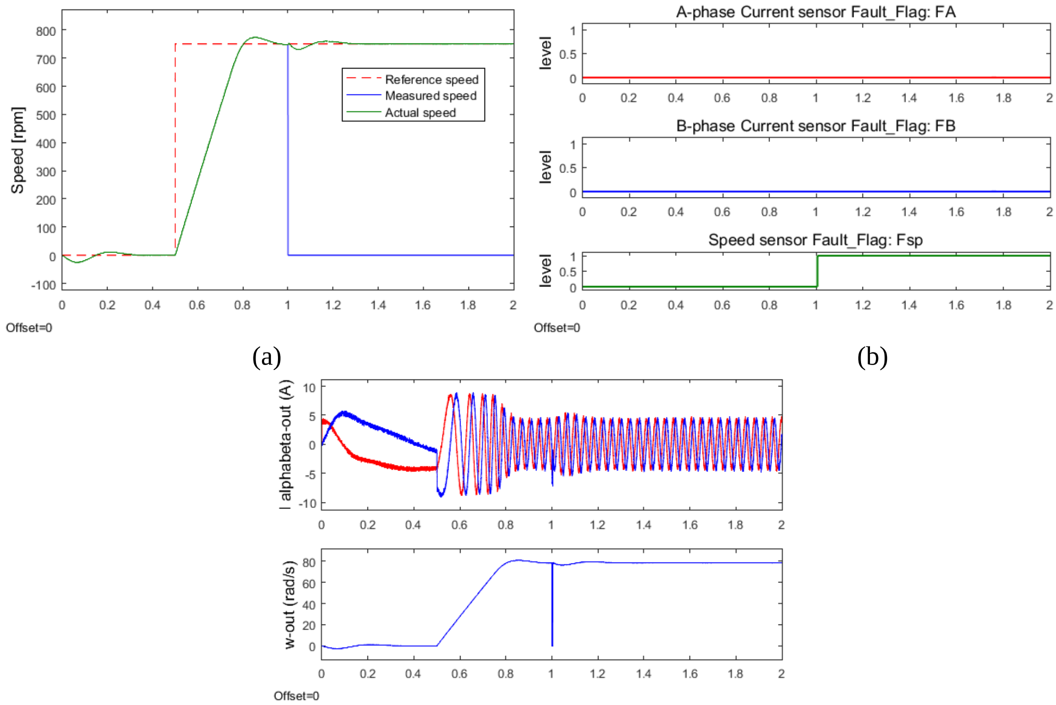

Figure 4. Speed fault case: (a) rotor speeds, (b) fault indication flags, (c) output signals of FDI.

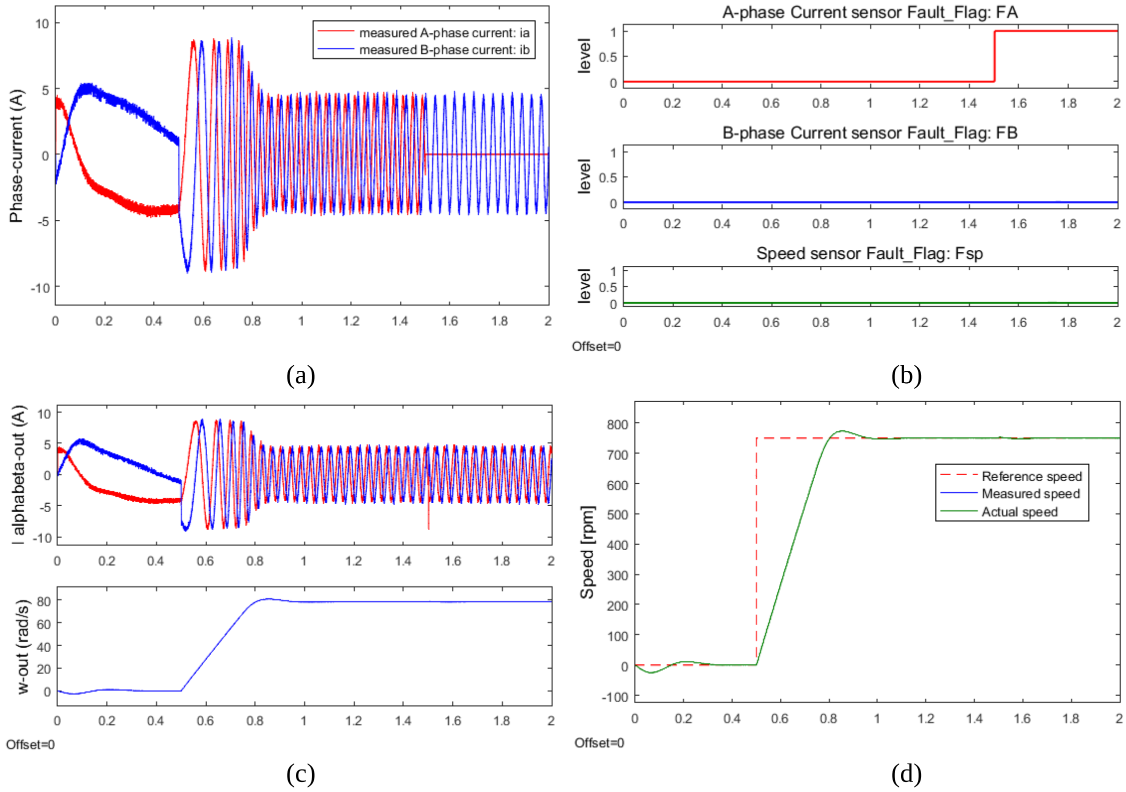

Figure 5. A-phase current fault case: (a) measured stator current, (b) fault indication flags, (c) output signals of FDI, (d) rotor speeds.

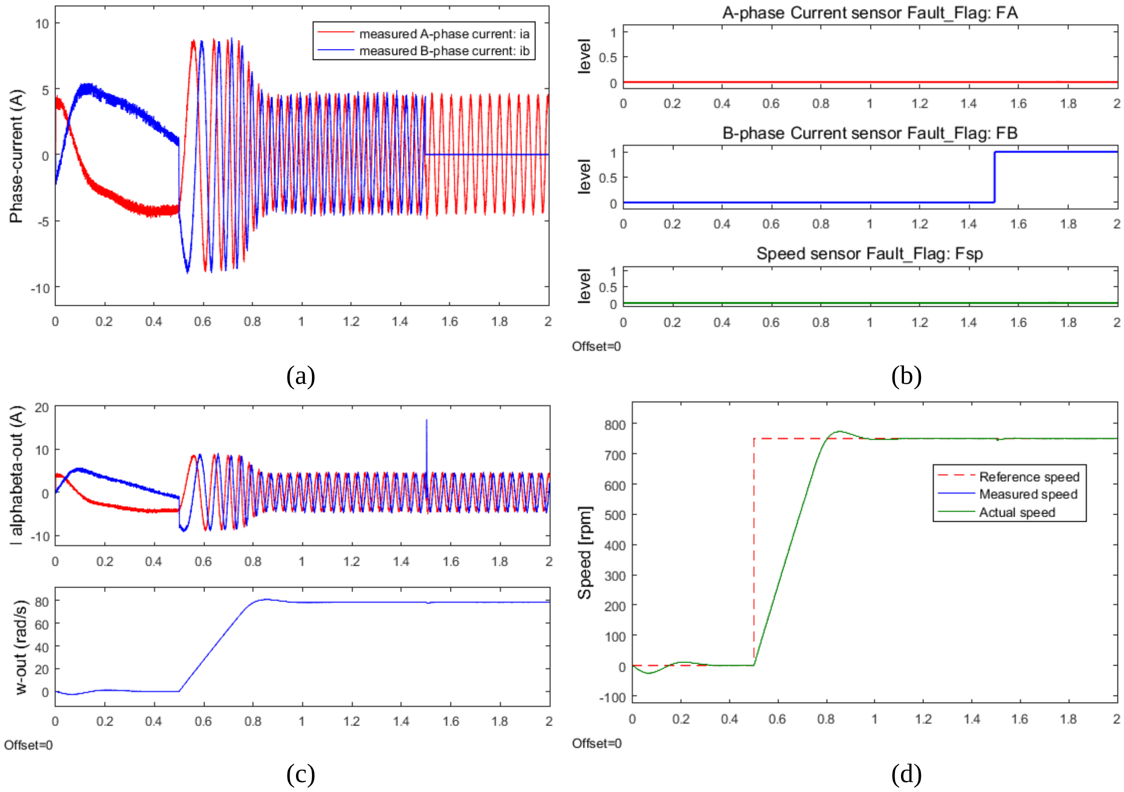

Figure 6. B-phase current fault case: (a) measured stator current, (b) fault indication flags, (c) output signals of FDI, (d) rotor speeds.

4. CONCLUSION

This paper presents an improved sensor fault-tolerant solution applied to the IMDs by using mathematical functions against the fault current and speed sensor. In the diagnosis algorithm, the current sensor's status is determined priority; then, the speed sensor's status will be checked for the FDI unit to make appropriate decisions. The FTC function can work correctly without confusion in detecting sensor failures. The loss of signal from the sensor will be quickly detected by the proposed FTC function and maintain the stable operation of the IDM when the sensor is disconnected or completely damaged. Compared with FTC methods based on the RMS technique, the advantage of the proposed FTC method is the fast fault detection time; sensor failures are almost immediately detected and determined, whereby the steady state of the speed control is quickly re-established under the operating sensorless mode. The fault-tolerant control method has proven effective against sensor failures and improved the IDM system's reliability. The feasibility of the proposed method has been demonstrated through simulation results with a speed sensor and two current sensor faults.

ACKNOWLEDGMENTS

This research is funded by Ton Duc Thang University, Vietnam, 2022-2023, under grant number FOSTECT.2022.05.

REFERENCES

[1] T. F. Chan and K. Shi, *Applied Intelligent Control of Induction Motor Drives*, 1st edition, Wiley and Sons, 2011.

[2] A. M. Trzynadlowski, *Control of Induction Motors*, 1st edition, Engineering & Transportation, 2000.

[3] T. Torres, J. Carlos, and M. A. Duarte-Mermoud. "Normalized Model Reference Adaptive Control Applied to High Starting Torque Scalar Control Scheme for Induction Motors," *Energies*, vol. 15, no. 3, 2022.

[4] K. Lee and Y. Han, "Reactive-Power-Based Robust MTPA Control for v/f Scalar-Controlled Induction Motor Drives," *IEEE Transactions on Industrial Electronics*, vol. 69, no. 1, pp. 169-178, 2022.

[5] Z. Zhang, *et al.*, "Robust Sensorless Scalar Control of Induction Motor Drives with Torque Capability Enhancement at Low Speeds," *IEEE International Electric Machines & Drives Conference (IEMDC)*, pp. 1706-1710, 2019.

[6] AN2388 Application note, "Sensor field oriented control (IFOC) of three-phase AC induction motors using ST10F276," ST Microelectronics, Oct. 2006, pp. 54.

[7] W. Li, *et al.*, "Induction Motor Control System based on FOC Algorithm," *IEEE International Information Technology and Artificial Intelligence Conference (ITAIC)*, pp. 1544-1548, 2019.

[8] D. L. Mon-Nzongo, T. Jin, G. Ekemb, and L. Bitjoka, "Decoupling Network of Field-Oriented Control in Variable-Frequency Drives," *IEEE Transactions on Industrial Electronics*, vol. 64, no. 7, pp. 5746-5750, 2017.

[9] M. Boukhnifer, *et al.*, "Fault Tolerant Control to Mechanical Sensor Failures for Induction Motor Drive: A Comparative Study of Voting Algorithms," *Annual Conference of the IEEE Industrial Electronics Society*, pp. 2851-2856, 2013.

[10] J. Azzoug, Y. Pusca, R. Sahraoui, M. Ammar, A. Ameid, T. Romary, and R. Cardoso, "An Active Fault-Tolerant Control Strategy for Current Sensors Failure for Induction Motor Drives using a Single Observer for Currents Estimation and Axes Transformation," *European Journal of Electrical Engineering*, vol. 23, No. 6, pp. 467-474. 2021.

[11] K. Klimkowski and M. Dybkowski, "A Fault Tolerant Control Structure for an Induction Motor Drive System," *Automatika*., vol. 57, no. 3, 2016.

[12] D. Diallo, M. E. H. Benbouzid, and M. A. Masrur, "Special Section on Condition Monitoring and Fault Accommodation in Electric and Hybrid Propulsion Systems," *IEEE Transactions on Vehicular Technology*, vol. 62, no. 3, pp. 962-964, 2013.

[13] M. Bouakoura, N. Nait-Said, M. S. Nait-Said, and A. Belbach, "Novel speed and current sensor FDI schemes with an improved AFTC for induction motor drives," *Advances in Electrical and Electronic Engineering*, vol. 16, no. 1, pp. 1-14, 2018.

[14] T. A. Najafabadi, F. R. Salmasi, and P. Jabehdar-Maralani, "Detection and Isolation of Speed, DC-Link Voltage and Current-Sensor Faults Based on an Adaptive Observer in Induction-Motor Drives," *IEEE Transactions on Industrial Electronics*, vol. 58, no. 5, pp. 1662-1672, 2011.

[15] C. Chakraborty and V. Verma, "Speed and Current Sensor Fault Detection and Isolation Technique for Induction Motor Drive Using Axes Transformation," *IEEE Transactions on Industrial Electronics*, vol. 62, no. 3, pp. 1943-1954, 2015.

[16] F. R. Salmasi, "A Self-Healing Induction Motor Drive with Model Free Sensor Tampering and Sensor Fault Detection, Isolation, and Compensation," *IEEE Transactions on Industrial Electronics*, vol. 64, no. 8, pp. 6105-6115, 2017.

[17] C. D. Tran, P. Brandstetter, M. C. H. Nguyen, S. D. Ho, B. H. Dinh, and P. N. Pham, "A Robust Diagnosis Method for Speed Sensor Fault based on Stator Currents in The RFOC Induction Motor Drive," *International Journal of Electrical and Computer Engineering*, vol. 10, no. 3, pp. 3035-3046, 2020.

[18] C. D. Tran, M. Kuchar, M. Sobek, V. Sotola, and B. H. Dinh, "Sensor Fault Diagnosis Method Based on Rotor Slip Applied to Induction Motor Drive," *Sensors*, vol. 22, no. 22, pp. 8636, 2022.

[19] S. P. Ganjewar and Y. Pahariya, "Modified MRAS Approach for Sensorless Speed Control of Induction Motor for Reliability Improvement," *International Journal of Information Technology*, vol. 14, pp. 1595–1602, 2022.

[20] P. Brandstetter and M. Dobrovsky, "Speed estimation of induction motor using model reference adaptive system with Kalman filter," *Advances in Electrical and Electronic Engineering*, vol. 11, no. 1, pp. 22-28, 2013.
[21] M. S. Zaky, M. K. Metwaly, H. Z. Azazi, and S. A. Deraz, "A New Adaptive SMO for Speed Estimation of Sensorless Induction Motor Drives at Zero and Very Low Frequencies," *IEEE Transactions on Industrial Electronics*, vol. 65, no. 9, pp. 6901-6911, 2018.
[22] C. S. T. Dong, C. D. Tran, S. D. Ho, P. Brandstetter, and M. Kuchar, "Robust Sliding Mode Observer application in Vector Control of Induction Motor," *Elektro.*, pp. 1-5, 2018.
[23] C. D. Tran, P. Brandstetter, M. H. Nguyen, S. D. Ho, P. N. Pham, and B. H. Dinh, "An Improved Current-Sensorless Method for Induction Motor Drives applying Hysteresis Current Controller," *Indonesian Journal of Electrical Engineering and Informatics (IJEEI)*, vol. 9, no. 1, pp. 130-140, 2021.
[24] V. Verma, "Current Sensorless Vector Controlled Induction Motor Drive," *International Journal of Robotics and Automation (IJRA*), vol. 8, no. 1, pp. 52-67, 2019.
[25] Y. Azzoug, *et al.*, "A Single Observer for Currents Estimation in Sensor's Fault-Tolerant Control of Induction Motor Drives," *International Conference on Applied Automation and Industrial Diagnostics (ICAAID)*, pp. 1-6, 2019.
[26] Y. Azzoug, M. Sahraoui, R. Pusca, T. Ameid, R. Romary, and A. J. M. Cardoso, "High-Performance Vector Control without AC Phase Current Sensors for Induction Motor Drives: Simulation And Real-Time Implementation," *ISA Transactions*, vol. 109, pp. 295-306, 2020.
[27] M. Adamczyk and T. Orlowska-Kowalska, "Self-Correcting Virtual Current Sensor based on the Modified Luenberger Observer for Fault-Tolerant Induction Motor Drive," *Energies*, vol. 14, no. 20, pp. 6767, 2021.
[28] Q. S. Vu, C. D. Tran, B. H. Dinh, C. S. T. Dong, H. T. Huynh, and H. X. Phan, "A Current Sensor Fault Diagnosis Method based on Phase Angle Shift Technique applying to Induction Motor Drive," *International Journal of Power Electronics and Drive Systems (IJPEDS)*, vol. 13, no. 3, pp. 1315-1325, 2022.

BIOGRAPHY OF AUTHORS

Minh Chau Huu Nguyen is a lecturer in the Faculty of Electrical-Electronics Engineering at Vietnam Aviation Academy. He graduated from the Military Technical Academy, Vietnam, and received his ME degree in Automation Engineering in 2012. He is researching at the Faculty of Electrical Engineering & Computer Science, VSB – Technical University of Ostrava, Czech Republic. His research interests include automatic control systems, intelligent control systems, electrical machines, apparatus, and drives. He can be contacted at email: minhnhc@vaa.edu.vn.

Cuong Dinh Tran is a lecturer in the Faculty of Electrical-Electronic Engineering at Ton Duc Thang University. He received his BE, and ME degrees from Ho Chi Minh City University Of Technology, Vietnam, and his Ph.D. from VSB-Technical University of Ostrava, the Czech Republic, in 2005, 2008, and 2020. His research interests include the field of modern control methods and intelligent algorithms in motor drives. He can be contacted at email: trandinhcuong@tdtu.edu.vn.